MECHANICS OF ROULEAU FORMATION

R. SKALAK, *Department of Civil Engineering and Engineering Mechanics, Columbia University, New York 10027*
P. R. ZARDA, *Martin-Marietta Aerospace Corporation, Orlando, Florida 32805*
K.-M. JAN AND S. CHIEN, *Department of Physiology, College of Physicians and Surgeons, Columbia University, New York 10032*

ABSTRACT The formation of rouleau of red blood cells is considered from the standpoint of adhesion theory. With the use of the elastic properties of the red blood cell membrane obtained from previous work, the strain energy of the red blood cell in rouleau formation has been computed. The surface energy of adhesion for the bonding of two red blood cells is then computed from the variation of this strain energy. Computed cell shapes agree well with experiments.

INTRODUCTION

The formation of rouleau of red blood cells has been extensively studied from the standpoint of the molecular forces which cause or prevent aggregation. (Jan and Chien, 1973*a*, *b*; Chien, 1976). The theory of the interaction of such adhesive forces with the elasticity of the red blood cell was previously developed by Skalak et al. (1977) and a similar analysis has been developed by Evans (1980) for the interpretation of pipette aspiration experiments. In the present paper computations of rouleau formation are carried out for a wider range of adhesive energies and geometries than previously presented. These computations allow estimates of the surface energy involved in rouleau formation based on a knowledge of the elastic properties of the cells and observed geometry of the rouleau. The pertinent theoretical equations are recapitulated in the next section and then the numerical results are presented.

THEORY

The basic ideas used to discuss rouleau are found in the theory of fracture originating with the work of Griffith (1921). Similar theory for the adhesion of two elastic bodies was discussed by Williams (1971). It is assumed that to separate two adhering surfaces a certain amount of work must be done to overcome molecular level forces. This is the surface energy γ (ergs/cm^2 or dyn/cm), which plays the role of the fracture or adhesive energy of a single material.

A general dynamic statement of conservation of energy may be made for rouleau formation (Skalak et al., 1977):

$$\frac{dU}{dt} = \frac{dW}{dt} + \frac{dT}{dt} + \frac{dD}{dt} - \gamma \frac{dA_c}{dt}, \tag{1}$$

where dU/dt is the rate of work done by external forces, which may include surface forces and body forces; dW/dt is the rate of increase of elastic stored energy (strain energy); dT/dt is the time rate of change of kinetic energy of the system; dD/dt is the rate of dissipation of energy

in the system, which may include viscous behavior of the solids as well as the fluids or dissipation in adhesion process itself; and $-\gamma(dA_c/dt)$ is the rate at which energy must be supplied to separate the contact surfaces, whose common area of contact is A_c.

The surface or adhesive energy γ is defined by

$$\gamma = \int_{y_0}^{\infty} \sigma_n \, dy, \tag{2}$$

where σ_n is the net force between two opposing membrane surfaces and y_0 is their equilibrium spacing.

The dynamic Eq. 1 would be useful when considering the effects of gravity or shear stress that augment or hinder rouleau formation. In the present case, only steady static positions will be considered, so that the kinetic energy term, the viscous dissipation, and the work done by external forces in Eq. 1 may be neglected.

The equilibrium positions studied here may be shown to correspond to stationary (usually minimum) values of the appropriately defined total potential energy P_T (Skalak et al., 1977):

$$\delta (P_T) = 0, \tag{3}$$

where

$$P_T = P - \gamma A_c, \tag{4}$$

and P is the potential energy of the system:

$$P = \int\int\int_R (W - F_i U_i) \, dV - \int\int_S T_i U_i \, dS, \tag{5}$$

where F_i are body forces and T_i are surface tractions. In the present case F_i and T_i are assumed to be zero. In treating the adhesion of two erythrocytes held by micropipettes, Evans (1980) has used a similar minimum principle, retaining the surface integral in Eq. 5 to account for the work done by the pipette pressures. In the case of rouleau formation treated here, the above Eqs. 3 and 4 lead to the equilibrium condition

$$\frac{dP_T}{dA_c} = 0 \text{ and hence } \gamma = \frac{dP}{dA_c}. \tag{6}$$

Using Eq. 5 with F_i and T_i zero, we can write Eq. 6 as (Skalak et al., 1977)

$$\gamma = \frac{\partial W}{\partial A_c}. \tag{7}$$

In Eq. 7, W is the elastic strain energy of the erythrocytes, and will vary with the contact area A_c. For each A_c, the equilibrium position of the rest of the cell is, in turn, the shape yielding a minimum W, when A_c is held constant. Such shapes may be found using methods developed previously (Zarda et al., 1977).

COMPUTATIONAL PROCEDURE

To make use of Eq. 7 in computations, the elastic strain energy function W must be known. In the present computations the elasticity of the erythrocyte is assumed to be due to the elastic properties of the

membrane only. The internal fluid is assumed to be incompressible. Further, the membrane is assumed to have constant surface area, which is the two-dimensional analog of an incompressible fluid. The elastic strain energy then arises only from shear deformations in the plane of the membrane and from bending stiffness associated with changes in curvature. The membrane energy is taken to be (Skalak et al., 1973)

$$W_M = \frac{B}{8}(I_1^2 + 2I_1 - 2I_2) \tag{8}$$

where I_1 and I_2 are the strain invariants:

$$I_1 = \lambda_1^2 + \lambda_2^2 - 2 \tag{9}$$

$$I_2 = \lambda_1^2 \lambda_2^2 - 1, \tag{10}$$

where λ_1 and λ_2 are the principal extension ratios. The coefficient B in Eq. 8 is an elastic shear modulus taken to be 0.005 dyn/cm for the erythrocyte membrane. The strain energy Eq. 8 has both quadratic and fourth power terms in the stretch ratios. At large stretch ratios, the presence of the fourth power term in Eq. 8 is not well supported by experimental pipette data, but its presence has little influence on the computations reported here because the maximum stretch ratios involved are only ~ 1.2.

The bending strain energy is taken to be of the form (Zarda et al., 1977):

$$W_B = D(K_1^2 + 2\nu K_1 K_2 + K_2^2)/2, \tag{11}$$

where K_1 and K_2 are changes in the principal curvatures, D is a bending stiffness, and ν is a material coefficient analogous to Poisson's ratio. The values of the constants used for the erythrocyte are $D = 10^{-12}$ dyn-cm and $\nu = 1/2$. Evans (1980) has estimated on the basis of pipette experiments that the value of $D = 10^{-12}$ dyn-cm is an upper bound for erythrocytes.

In the computations presented here, the erythrocytes are assumed to be axisymmetric before and after deformation. Two cases are treated in detail. The first is a rouleau consisting of only two cells. In the second case, a typical cell in the interior of a long straight rouleau is considered. In both cases, the symmetry of the problem suggests that it is sufficient to treat only one cell computationally and that the surface of adhesion common to two adjacent cells is a plane. This last assumption is reasonable for low surface energies, but, as will be shown in the results, is probably not valid for high energies which produce curved surfaces of contact.

The computations are carried out by a finite-element method that is described in detail in Zarda et al. (1977). Since the cases treated are axisymmetric, the method deals with the typical cross-section of the

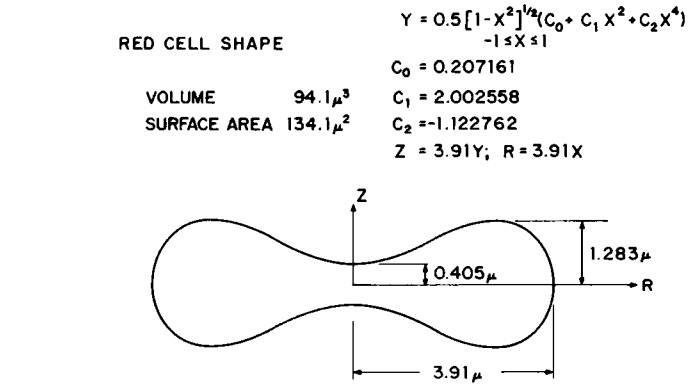

FIGURE 1 Unstressed shape assumed for human erythrocyte (Evans and Fung, 1972).

cell in a radial plane. The curve representing the cell surface is located by a number of nodes (usually 25–50) and suitable interpolation functions between nodes in each element, made up of five successive nodes. In the computations reported here, the contact area A_c is specified in advance and the shape of the rest of the cell is computed by the finite element method. This involves a Newton-Raphson iteration procedure in which the position of each node of the membrane is varied until a minimum of the strain energy W is found for the assumed value of contact area A_c. After carrying out such computations for a range of values of A_c, Eq. 7 is then used to determine the adhesive surface energy at each value of A_c.

NUMERICAL RESULTS

The equilibrium shape of the erythrocyte cross section used in these computations is shown in Fig. 1, based on Evans and Fung (1972). The equilibrium shapes computed for two-cell rouleau are shown in Fig. 2. Only one-half of one of the two cells of each rouleau is shown, as the rest of the cells are mirror images with respect to the radial (vertical) and axial (horizontal) coordinate axes. The initial shape is shown just touching the vertical plane (z = 0). This plane is the assumed surface of contact of the two-cell rouleau.

The contact area A_c in each case shown in Fig. 2 is fixed in advance by specifying the radius R_0 of the plane disk of contact, as indicated in the figure. After each shape is computed, the total strain energy $W = W_B + W_M$ is computed for one complete cell. The adhesive energy γ is

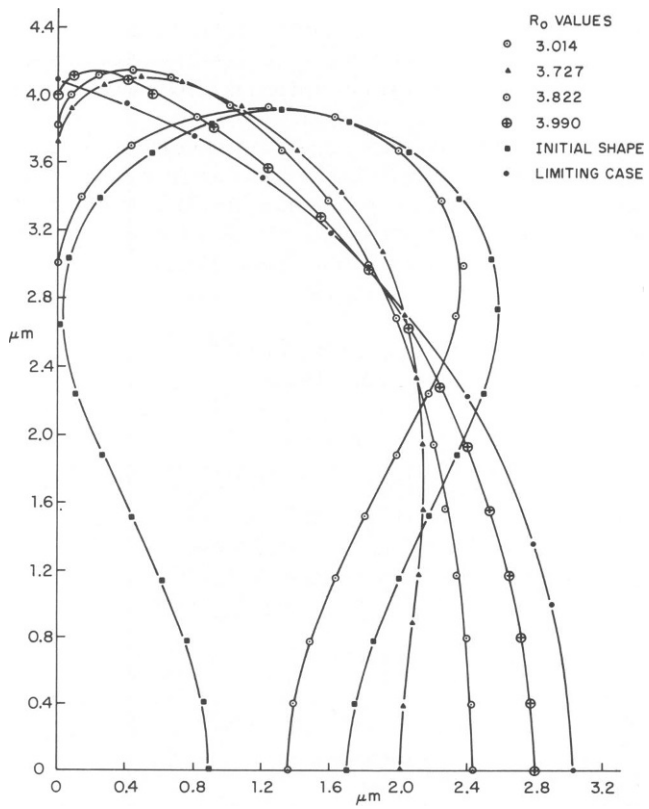

FIGURE 2 Computed shapes of one cell of a two-cell rouleau or the end of a long rouleau.

then computed for each value of the contact radius by using Eq. 7 in the form

$$\gamma = \frac{\partial(2W)}{\partial A_c} = \frac{1}{\pi R_0} \frac{\partial W}{\partial R_0}, \tag{12}$$

where W is the total strain energy for one cell; $2W$ is used in Eq. 12 for the two identical cells in contact. The derivative in Eq. 12 was evaluated by a finite difference approximation using the discrete values of R_0 for which equilibrium shapes were computed.

The results for the adhesive energy γ vs. R_0 are shown in Fig. 3. It may be seen in Fig. 2 that there is limiting case as $R_0 = 4.10$ μm is approached, for which the adhesive energy required approaches infinity. This is due to sharp curvature required near the outer edge of the cell. The limiting case shown in Fig. 2 is made up of a flat disk ($R_0 = 4.10$ μm) and a segment of a spherical surface. The radius of the spherical surface is $r_s = 4.29$ μm. These dimensions give the maximum value of R_0 such that the area and volume of the cell remain at their initial values shown in Fig. 1. It can be proved that the limiting outer surface must be a portion of a sphere. In Fig. 2 it can be seen that the numerical computations are approaching the theoretical limiting shape as R_0 is increased.

In carrying out the computations for Figs. 2 and 3, the pressure inside the cell is treated as an unknown, except for the unstressed position, for which the pressure is assumed to be zero. For any other shape, the internal pressure of the cell is adjusted so that the cell volume remains fixed. A plot of the pressure vs. the contact radius R_0 is shown in Fig. 4. It may be

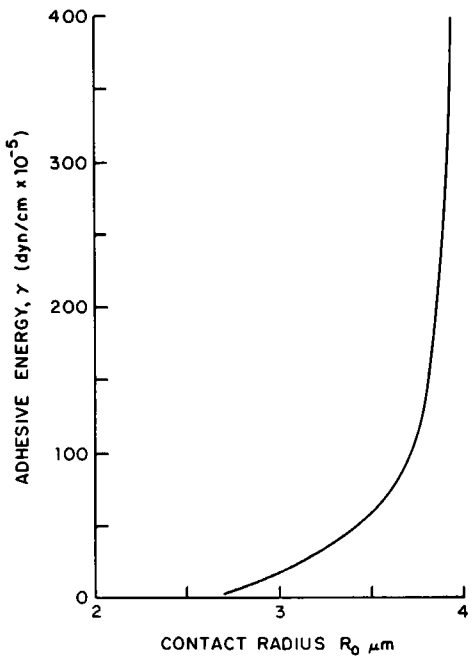

FIGURE 3 The adhesive energy required for end cell (or two-cell rouleau) as a function of the radius R_0 of adhered disk area.

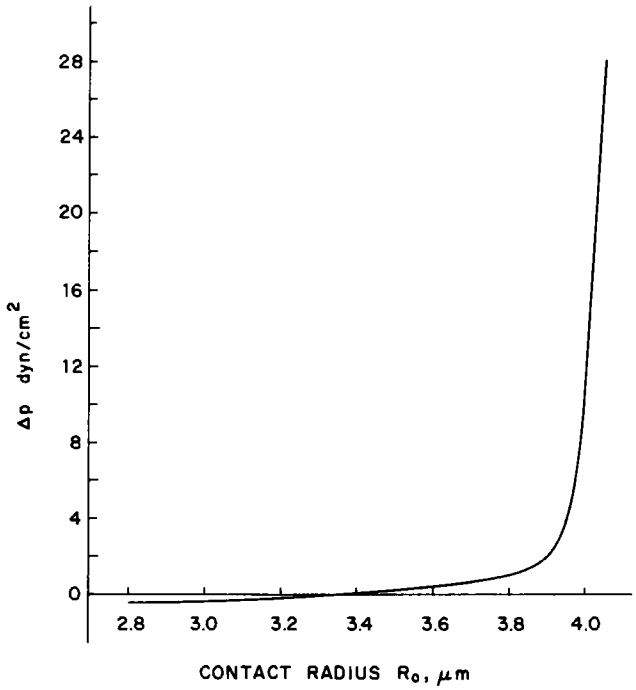

FIGURE 4 Pressure inside of end cell of a rouleau corresponding to the computed shapes shown in Fig. 2.

seen that the internal pressure approaches infinity as the contact radius approaches its limiting value.

Consider next the case of an erythrocyte in the interior of a long rouleau. Photomicrographs show that such rouleau are quite regular and most cells appear to be axisymmetric and also appear to be symmetric with respect to a plane that bisects the cell and is normal to the axis of rouleau. Assuming such symmetry, we need only treat one-quarter of the cell, as in Fig. 5. The plane of symmetry is chosen as $z = 0$. In the computations, the boundary condition enforced at $z = 0$ is that the tangent plane to the membrane remain parallel to the z-axis, but the radial coordinate is left free, to be determined by equilibrium equations. The right-hand boundary of the half-cell shown in Fig. 5 is assumed to be the contact area with the neighboring cell. This contact area is again assumed to be plane and normal to the z-axis.

The computation proceeds in a manner similar to that of the end cell. The value of the contact radius R_0 is assumed and the equilibrium shape is computed by the finite element program. The internal pressure of the cell is again adjusted so as to keep the volume of the cell constant. One further condition is required in the present case, that the total axial force be zero. This requirement assumes that the rouleau is freely floating and neutrally buoyant in a liquid at rest. Under these conditions, equilibrium requires a zero axial force. For any section through the cell, this force is made up of the tensions in the membrane plus the pressure force exerted by the fluid inside the cell. The finite element program is arranged for this computation so that this zero axial force condition is automatically satisfied by each solution computed. This is done by appropriate adjustment of the width of the cell in the z direction.

The shapes of the interior cells of a long rouleau computed for various assumed contact

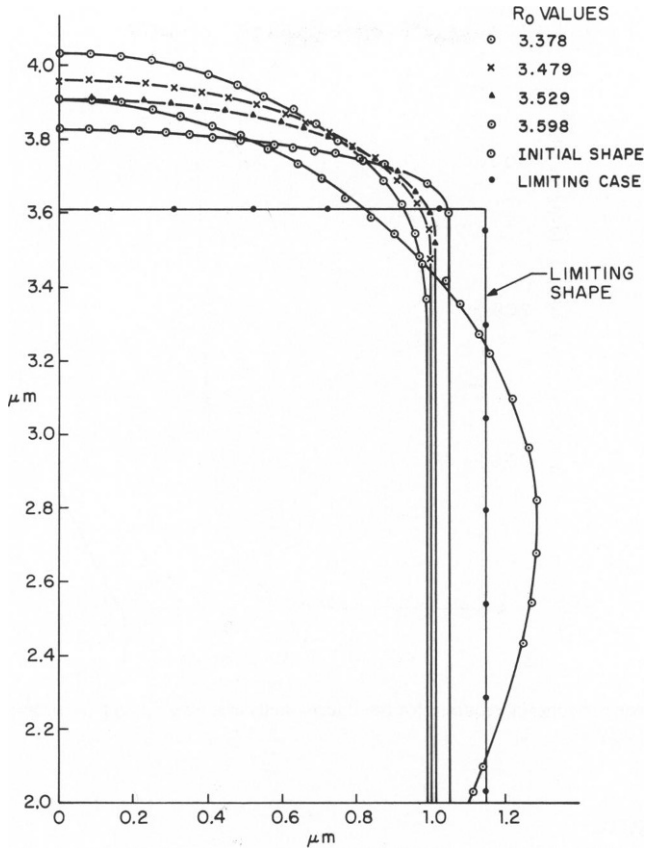

FIGURE 5 Computed shapes of cells in the middle of a long rouleau as a function of the radius R_0 of the adhered disk area.

radii, R_0, are shown in Fig. 5. The pressure computed inside the cell is a similar function of R_0, as in Fig. 4. This pressure approaches infinity as the value of R_0 approaches its limiting value. For the present case, the maximum value of R_0 is the radius of a cylinder such that the surface and volume of each cell retain the initial values shown in Fig. 3. The limiting value of R_0 is 3.61 μm.

After the equilibrium shapes are found, the value of the adhesive energy γ required for each R_0 assumed is detrmined by use of Eq. 7. In this case, the appropriate strain energy is that computed for one whole cell (i.e., two halves, one from each adjacent cell of a given contact area). Then in this case,

$$\gamma = \frac{\partial W}{\partial A_c} = \frac{1}{2\pi R_0} \frac{\partial W}{\partial R_0}, \tag{13}$$

where W stands for the total strain energy of one complete cell with contact radius R_0. Values of γ computed as a function of R_0 by finite differences are shown in Fig. 6. It can be seen that as the limiting case of a cylindrical shape is approached the value of γ approaches infinity, owing to the sharp curvature required near the junction of the neighboring cell membranes.

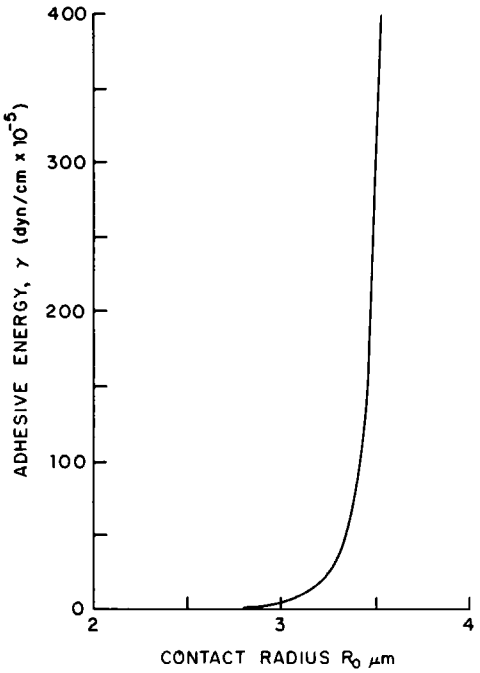

FIGURE 6 The adhesive energy required for the interior cells of a long rouleau as a function of the radius R_0 of the adhered disk area.

DISCUSSION

In the present theory and computations, the adhesion energy γ has been derived from known elastic properties of the erythrocyte membranes. A quantitative confirmation of the adhesion energy for specific agents causing rouleau formation could be achieved if the adhesive forces at a molecular level were known, so that Eq. 2 could be evaluated. The net force σ_n in Eq. 2 is the resultant of electrostatic repulsion and adhesive or bridging forces supplied by the bonding agent (Jan and Chien, 1973*a, b*). The variation of the electrostatic repulsion is fairly well known (Jan and Chien, 1973*a, b*) but the variation of the bonding molecular forces with the distances between membranes is not known. Consequently, it is not feasible to obtain reliable estimates of γ by the direct use of Eq. 2 at this time.

Qualitative confirmation of the computed results presented here can be seen by comparison with experimental observations of the shapes of erythrocytes in rouleau produced by varying the composition of the suspending medium. For example, if rouleau are formed in suspending media with various concentrations of dextran, the adhesive energy increases with increasing dextran concentration at first. Later, by a volume exclusion effect that causes an increase in electrostatic repulsion (Chien and Jan, 1973; Jan and Chien, 1973*a,b*) increasing concentration of dextran results in a decrease in adhesive energy. In Fig. 7 are shown rouleaux formed by two different concentrations (1 and 4 g/100 ml) of dextran (Dx) with a molecular weight of 74,500 (Dx 70). It can be seen that the outer face of the end cell is at first concave and then becomes convex. At the higher concentrations (e.g., 6 g/100 ml), it becomes concave again.

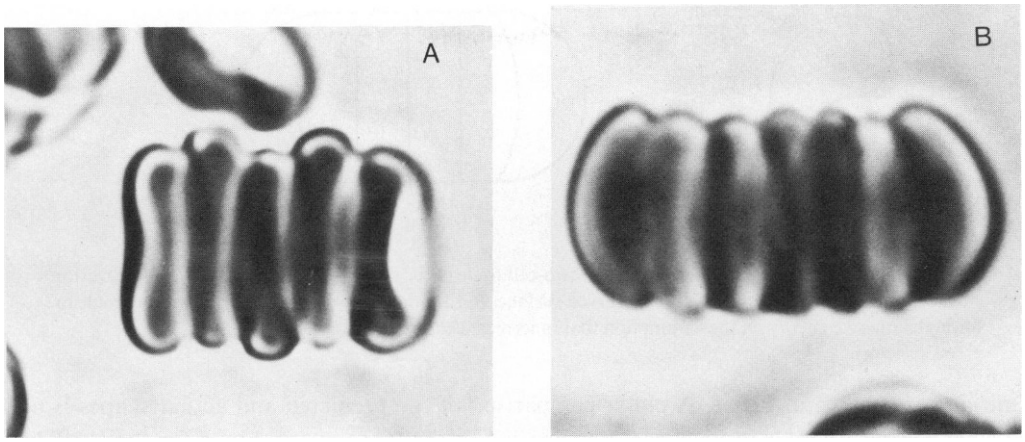

FIGURE 7 *A*, Photomicrograph of a rouleau formed in a suspension with Dextran Dx 70 (mol wt 75,000) present at a concentration of 1 g/100 ml. Note that the end cell is concave. *B*, Photomicrograph of a rouleau formed in a suspension with Dextran Dx 70 (mol wt 75,000) at a concentration of 4 g/100 ml. Note that the end cell is convex.

This corresponds to the sequence of shapes to be expected from Fig. 2 for increasing and then decreasing the adhesive energy.

Another qualitative feature of agreement of the theory and experimental observations is that in long rouleau it may be observed experimentally that for increasing adhesive energy, the shape of the rouleau is very nearly cylindrical of uniform diameter, approaching the

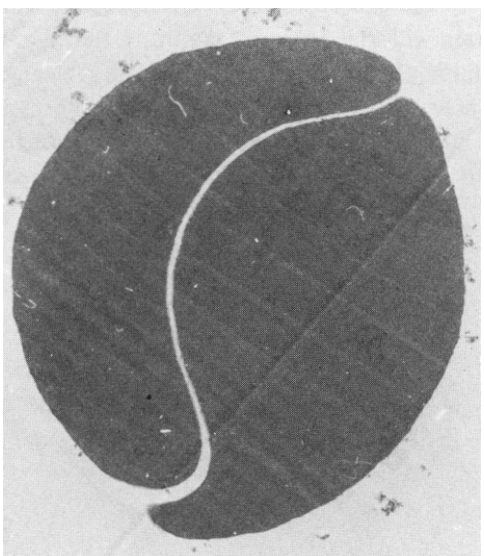

FIGURE 8 Electronmicroscopic cross-section of a rouleau formed in a suspension containg Dextran Dx 70 (mol wt 75,000) at a concentration of 4 g/100 ml. Note that interior cell boundaries are curved. (Magnification 22,000 x.)

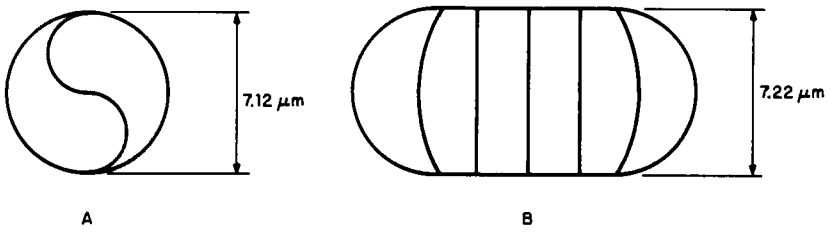

FIGURE 9 *A*, Limiting shape computed for a two-cell rouleau for very high adhesive energy. The exterior surface is a sphere. The contact area is a curved surface. *B*, Limiting shape computed for a six-cell rouleau for high adhesive energy on the assumption that innermost cells are cylindrical disks.

limiting case shown in Fig. 5. A closer comparison of the predicted and actual shapes is not possible because there is insufficient variation in the shapes shown in Fig. 5 for the available range of adhesive forces and the resolution required is beyond the capability of light microscopy.

The end cells of long rouleau observed experimentally appear to approach a hemispherical shape with a maximum diameter slightly less than the maximum diameter of the unstressed erythrocyte, as shown in Fig. 7*B*. The limiting case shown in Fig. 2 is not observed experimentally because the interior contact surface assumed to plane in the theoretical solutions is actually a curved surface at high adhesive energies, as shown by the photomicrograph in Fig. 8. The present theory could reproduce such shapes by allowing the contact surface to be curved. In this case, the resulting surfaces are not axisymmetric which complicates the computational procedures.

Limiting cases of very high adhesive energies can be readily computed from the general principle that in such cases the exposed surface area will be a minimum for the enclosed volume and the contact area will thus be a maximum. In the case of a two-cell rouleau, the limiting sphere is shown in Fig. 9*A*. If it is assumed that the rouleau exists in cylindrical form, the limiting case is as shown in Fig. 9*B*. This cylindrical form is probably unstable for sufficiently high adhesive energies. A spherical clump of cells maximizes the contact area. A photomicrograph of a nearly spherical clump of a number of erythrocytes is shown in Fig. 10.

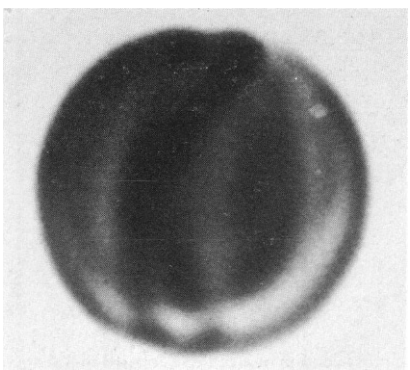

FIGURE 10 Photomicrograph of a group of erythrocytes under large adhesive energy. The spherical clump maximizes contact area between cells.

In such cases, the adhesive energy term in Eq. 4 predominates and the elastic strain energy is negligible. At lower adhesive energies the more cylindrical form of rouleau is usually found experimentally. This implies that the cylindrical form corresponds to a minimum of the total potential, taking into account the elastic strain energy of the cells.

The numerical results in Figs. 3 and 6 imply that rouleau may be formed over a wide range of surface adhesion energies. This is because small deformations of erythrocytes may be accomplished with little energy input. Thus Figs. 3 and 6 suggest that rouleau may be expected with adhesion energies as low as 10^{-4} dyn/cm. In the mid-range of these graphs γ is of the order of 2×10^{-3} dyn/cm. This is the same order of magnitude as computed from erythrocytes held in micropipettes (Evans, 1980). After bringing the cells into contact, fairly strong adhesions were computed to have an interfacial energy of $3–4 \times 10^{-3}$ dyn/cm. Thus, the two types of experiments give similar orders of magnitude for γ. In the rouleau formation, the exact extent of the contact area is not easily measured, so that precise values of γ are not readily predicted.

Received for publication 1 May 1980 and in revised form 12 March 1981.

REFERENCES

Chien, S., and K.-M. Jan. 1973. Ultrastructural basis of the mechanism of rouleaux formation. *Microvasc. Res.* 5:155–166.

Chien, S. 1976. Electrochemical interactions between erythrocyte surfaces. *Thromb. Res.* 8(Suppl. II): 189–202.

Evans, E. A. 1980. Minimum energy analysis of membrane deformation applied to pipette aspiration and surface adhesion of red blood cells. *Biophys. J.* 30:265–284.

Evans, E., and Y.-C. Fung. 1972. Improved measurements of the erythrocyte geometry. *Microvasc. Res.* 4:335–347.

Griffith, A. A. 1921. The phenomena of rupture and flow in solids. *Philos. Trans. R. Soc. Lond. A Math. Phys. Sci.* 221:163–198.

Jan, K.-M., and S. Chien. 1973*a*. Role of surface electric charge in red blood cell interaction. *J. Gen. Physiol.* 61:638–654.

Jan, K.-M., and S. Chien. 1973*b*. Influence of the ionic composition of fluid medium on red cell aggregation. *J. Gen. Physiol.* 61:655–668.

Skalak, R., A. Tözeren, P. R. Zarda, and S. Chien. 1973. Strain energy function of red blood cell membranes. *Biophys. J.* 13:245–264.

Skalak, R., P. R. Zarda, K.-M. Jan, and S. Chien. 1977. Theory of rouleau formation. *In* Cardiovascular and Pulmonary Dynamics. M. Y. Jaffrin, editor. Institut National de la Santé et de la Recherche Medical (INSERM) 77:299–308.

Williams, M. L. 1971. Applications of Continuum Mechanics in Adhesive Fracture. American Chemical Society, Organic Coatings Division, Washington, D.C.

Zarda, P. R., S. Chien, and R. Skalak. 1977. Elastic deformations of red blood cells. *J. Biomech.* 10:211–221.